frontiers | Frontiers in Immunology

TYPE Original Research
PUBLISHED 03 April 2025
DOI 10.3389/fimmu.2025.1550775

OPEN ACCESS

EDITED BY
Sheila Donnelly,
University of Galway, Ireland

REVIEWED BY
Arijit Bhattacharya,
Adamas University, India
Xuelian Bai,
Binzhou Medical University Hospital, China
Muhammad Imran,
University of Agriculture, Faisalabad, Pakistan

*CORRESPONDENCE
Yanwen Li
2506345708@qq.com
Dengyu Liu
33547533@qq.com

†These authors have contributed equally to this work and share first authorship

RECEIVED 24 December 2024
ACCEPTED 18 March 2025
PUBLISHED 03 April 2025

CITATION
Shi Y, Li X, Liang K, Lu T, Chen Y, Lai Y, Li Y, Wei S, He S, Tang L, Liu D and Li Y (2025) Characteristics and immunoprotective functions of three cysteine proteases from *Clonorchis sinensis*. *Front. Immunol.* 16:1550775. doi: 10.3389/fimmu.2025.1550775

Characteristics and immunoprotective functions of three cysteine proteases from *Clonorchis sinensis*

Yunliang Shi[1,2†], Xiaoqin Li[1,3†], Kai Liang[4], Ting Lu[1], Yu Chen[5], Yashi Lai[1], Yaoting Li[1], Shuai Wei[6], Shanshan He[1], Lili Tang[1], Dengyu Liu[1,2*] and Yanwen Li[1,2*]

[1]Parasitology Department, School of Basic Medical Sciences, Guangxi Medical University, Nanning, China, [2]Key Laboratory of Basic Research on Regional Diseases (Guangxi Medical University), Education Department of Guangxi Zhuang Autonomous Region, Nanning, China, [3]Department of Medical Laboratory, Shenzhen Longgang District Eighth People's Hospital, Shenzhen, China, [4]Gastroenterology Department, Guangxi Zhuang Autonomous Region People's Hospital, Nanning, China, [5]Department of Schistosomiasis Prevention and Control, Disease Prevention and Control Center of Hengzhou City, Hengzhou, China, [6]Department of Medical Laboratory, Hechi People's Hospital, Hechi, China

Introduction: Cysteine proteases from *Clonorchis sinensis*, including various proteins, are essential for its pathogenicity and serve as potential vaccine candidates. This study assesses the protective effects of three *C. sinensis* cysteine proteases (CsCP1-3).

Methods: Mice immunized with recombinant CsCP1-3 and adjuvants were subsequently infected with *C. sinensis* metacercariae after three immunization rounds. Liver damage was evaluated through hematoxylin and eosin (H&E), Masson's trichrome, and immunohistochemical analyses. The levels of IgG1, IgG2a antibodies, and cytokines (IFN-g, IL-2, IL-4, and IL-10) were quantified by enzyme-linked immunosorbent assay (ELISA).

Results: RT-qPCR revealed that CsCP1-2 exhibited the highest expression in newly encysted larvae (NEL), while CsCP3 was predominantly expressed in adult stages. Immunohistochemical localization confirmed that CsCP1-3 are present in the eggshells, syncytial layers of metacercariae, NEL cuticle, and adult intestines. Histological and immunohistochemical analysis demonstrated that the rCsCP1-3-immunized group displayed reduced liver inflammation and biliary fibrosis compared to the control group. The rCsCP1-3 induced a progressive increase in specific IgG1 and IgG2a antibody titers by the second week post-immunization. In the CsCP1-2 group, cytokines IFN-g, IL-2, IL-4, and IL-10 were elevated relative to the control, with particularly high levels of IFN-g and IL-10 in CsCP1, indicating a strong mixed Th1/Th2 immune response. In contrast, the CsCP3 immunization group exhibited a transient increase in cytokines (IFN-g, IL-2, IL-4, and IL-10) three days postinfection, which subsided after one to two weeks.

Discussion: These findings suggest that CsCP1-3 elicit robust antibody and cellular immune responses, mitigating liver damage caused by *C. sinensis* infection. CsCP1, in particular, induces a potent mixed Th1/Th2 response, positioning it as a promising vaccine candidate.

KEYWORDS

***Clonorchis sinensis*, cysteine proteases, characteristics, liver damage, immune protection**

1 Introduction

Clonorchiasis is a serious foodborne parasitic disease that affects over 200 million people worldwide, with an estimated 15-20 million individuals infected (1, 2). Infection with *Clonorchis sinensis* (*C. sinensis*) primarily occurs through the accidental ingestion of metacercariae, potentially leading to bile duct dilation, cholecystitis, cholelithiasis, liver fibrosis, and even hepatocellular carcinoma and cholangiocarcinoma (3–5). The disease is mainly endemic in southeastern and northeastern China, northern Korea, northern Vietnam, and eastern Russia, regions where the consumption of raw fish is common, complicating prevention and control efforts (6, 7). Current prevention and treatment strategies primarily rely on medications such as praziquantel and albendazole, with no commercially available vaccine yet (8, 9).

Cysteine proteases (CPs) are eosinophilic proteolytic enzymes with hydrolytic activity. They are classified into various families based on primary amino acid sequence and secondary/tertiary structure (10). In parasitic organisms, CPs are secreted proteins involved in key biological and pathogenic processes, including host cell adhesion, tissue invasion, cytotoxicity, nutrient uptake, and immune evasion (11, 12). CPs from various parasites have shown the potential to induce robust humoral and cell-mediated immune responses, positioning them as promising vaccine candidates (13). CPs derived from *Fasciola hepatica* (14), *Schistosoma mansoni* (15, 16), *Haemonchus contortus* (17), and *Trichinella spiralis* (18) have been demonstrated to stimulate strong immune responses, with immunization reducing worm burden (18, 19). As such, parasitic CPs are considered significant vaccine candidates with broad potential for application (20, 21).

Several cysteine proteases have been identified in *C. sinensis*, including cathepsins B, F, L, and legumain (22–25). However, limited immunoprotection studies on CsCPs have been conducted. Notably, a 37.6 kDa CsCP has been shown to induce both humoral and cellular immune responses, providing substantial protection in Sprague-Dawley rats (26). Additionally, a 35 kDa recombinant CsCP (B.s-CotC-CsCP) has demonstrated the ability to induce a specific immune response in mice, resulting in a significant reduction in liver fibrosis post-immunization (27). Furthermore, immunization with CotC-CsCP in grass carp has proven effective in conferring resistance to *C. sinensis* infection (28). Despite these findings, the immunoprotective roles of many CsCPs remain inadequately understood.

This study examines the expression and localization of three *C. sinensis* cysteine proteases (CsCP1-3). Mice were immunized with recombinant forms of these proteases and subsequently challenged with *C. sinensis* infection to assess liver damage and measure antibody and cytokine levels. This investigation into the immunoprotective roles of CsCP1-3 aims to enhance understanding of their potential as vaccine candidates.

2 Materials and methods

2.1 *C. sinensis* metacercariae, newly excysted juvenile worms, adult worms and eggs preparation

C. sinensis-infected *Pseudorasbora parva* was collected from Hengzhou City, Guangxi. After the head, scales, and viscera were removed, the fish flesh was minced and digested at 37°C for 12 hours in an artificial digestive fluid (1% hydrochloric acid and 0.6% pepsin). Metacercariae were isolated under a stereomicroscope and stored in 0.9% saline solution (29). A portion of the metacercariae was treated with trypsin digestive fluid (0.025% trypsin, pH 7.4) and incubated at 37°C for 3 minutes to obtain newly excysted juveniles (NEJ). Additionally, a portion of the metacercariae was orally administered to Sprague-Dawley (SD) rats, with 150 metacercariae per rat. After 4 weeks, the rats were euthanized, and adult worms were collected from the bile ducts, along with eggs from the uteri of the adult worms. The adult worms, NEJ, metacercariae, and eggs were partially stored in RNA preservation solution at -80°C and partially fixed in 4% paraformaldehyde at room temperature.

2.2 Expression, purification, and identification of recombinant CsCP1-3 protein

Total RNA was extracted from adult *C. sinensis*, and cDNA was synthesized through reverse transcription. The CsCP1-3 gene (GenBank Accession: DQ902582.1, DQ902583.1, DQ902586.1)

was amplified by PCR and subcloned into the pPic9k (+) expression vector(Sangon Biotech, Shanghai, China), creating the recombinant plasmid pPic9k (+)-CsCP1-3. After sequence verification, the construct was transformed into the *Pichia pastoris* GS115 strain (Sangon Biotech, Shanghai, China). GS115 cells harboring pPic9k (+)-CsCP1-3 were inoculated into 5 mL of YPD liquid medium and cultured at 30°C with shaking at 250 rpm for 12 hours. The culture was then diluted 1:50 into BMGY medium and further incubated at 30°C with shaking at 250 rpm for 12-16 hours. Following centrifugation at room temperature, the cells were resuspended in an equal volume of BMMY medium and cultured at 30°C with shaking at 250 rpm. Methanol was added every 12 hours to maintain a final concentration of 0.5%, and after 72 hours, the supernatant was collected by centrifugation at 4°C and analyzed by 12% SDS-PAGE and Western blotting. The expressed protein was purified using a Ni-agarose affinity column with a His tag and dialyzed to obtain a large quantity of the protein.

2.3 Preparation of anti-rCsCP1-3 immune sera

To generate anti-sera for subsequent experiments, 150 μg of rCsCP1-3 was mixed with an equal volume of complete Freund's adjuvant(Sigma-Aidrich, USA) and administered to rats *via* multiple subcutaneous and intradermal injections. The dose was halved for the second and third booster immunizations, which were given at 2-week intervals. Blood was collected from the rats' tails before each vaccination and 2 weeks after the final immunization (30). The serum was separated, inactivated by heating at 56°C for 30 minutes to deactivate the complement, and stored at -20°C for future use. The serum was initially diluted at 1:800 and further serially diluted, with the titer of anti-rCsCP1-3 serum determined using an ELISA method.

2.4 CsCP1-3 expression at different developmental stages of *C. sinensis*

Total RNA was extracted from the eggs, metacercariae, NEJ, and adult worms of *C. sinensis* using the Trizol method. cDNA was synthesized using the PrimeScript RT Master Mix kit (Takara, Japan, RR036A). Primers for CsCP1-3 were designed according to the information in Supplementary Table 1, with PCR amplification conditions specified therein. RT-qPCR was performed using the Takara RT-qPCR premix (RR820A, Japan), with β-Actin as the internal reference gene. Relative mRNA levels of CsCP1-3 at different developmental stages of the liver fluke were determined using the comparative cycle threshold (2−ΔΔCT) method (31).

2.5 Localization of CsCP1-3 in different developmental stages of *C. sinensis*

Eggs, metacercariae, NEJ, and adult worms of *C. sinensis* were fixed in 4% paraformaldehyde, paraffin-embedded, and sectioned to 4 μm thickness. The sections underwent deparaffinization using xylene and graded ethanol, followed by antigen retrieval in Sodium Citrate Antigen Retrieval Solution (pH 6.0) using an autoclave. Endogenous peroxidase activity was quenched with 3% H_2O_2 for 15 minutes, followed by incubation with 5% goat serum (1:10 dilution) at 37°C for 30 minutes. Subsequently, the sections were incubated overnight at 4°C in the dark with SD rat anti-CsCP1-3 serum (1:800 dilution). The following day, after equilibration to room temperature, the sections were washed four times with PBS, then incubated with Goat Anti-Rat IgG H&L (Alexa Fluor® 594) (Abcam, United Kingdom) at 37°C for 1 hour with intermittent shaking. After three PBS washes, protein localization was observed using a fluorescence microscope (Leica DMi8, Germany).

2.6 Immunization protocol with rCsCP1-3 protein

Eight-week-old BALB/c mice were randomly assigned to five groups, each comprising nine mice. The initial immunization involved administration of 75 μg of rCsCP protein (dissolved in 50 μL) mixed with 50 μL of complete Freund's adjuvant. For the second and third booster immunizations, incomplete Freund's adjuvant (Sigma-Aldrich, USA) was used, with the dosage reduced by half. The primary, secondary, and tertiary immunizations were administered at two-week intervals. Control groups received PBS or PBS plus Freund's adjuvant. Two weeks after the final immunization, each mouse was orally administered 30 metacercariae. At 0, 2, and 4 weeks post-gavage, three mice from each group were euthanized, and serum, spleen, and liver tissues were harvested for liver function assays, splenocyte culture, and histopathological analysis.

2.7 Histopathological assessment of liver tissue

For dehydration, liver tissues were fixed in 4% paraformaldehyde for 24 hours, followed by a graded ethanol dehydration series (70%, 80%, 90%, 95%, and 100%). After clearing with xylene, the tissues were embedded in paraffin, sectioned, and mounted. Sections were stained with hematoxylin and eosin (HE) for routine histological evaluation and Masson's trichrome for collagen visualization. Pathological alterations were examined and documented using a light microscope (Olympus BX43, Japan). Liver inflammation was quantified using the mHAI scoring system based on HE staining (32). Fibrotic areas were morphologically evaluated and scored using the Ishak scoring system with ImageJ software after Masson's trichrome staining (33).

For immunohistochemical analysis, antigen retrieval of mounted sections was achieved by incubation in citrate buffer (pH 6.0) for 3 minutes, followed by endogenous peroxidase blocking at room temperature for 10 minutes. After a 30-minute blocking step with 5% goat serum at 37°C, sections were incubated overnight at 4°C with primary antibodies: Anti-α-SMA Mouse mAb (1:1000 dilution) and Anti-Collagen I Rabbit pAb (1:1000

dilution) (both from Servicebio, Wuhan, China). Following washes, sections were incubated with HRP-conjugated secondary antibodies—Goat Anti-Mouse IgG (catalog number D110087-0100) and Goat Anti-Rabbit IgG (1:2000 dilution, catalog number D110058-0100) (both from Sangon Biotech, Shanghai, China)—for 45 minutes at 37°C. Immune complexes were visualized using 3,3'-diaminobenzidine (DAB), with subsequent hematoxylin counterstaining for 5 minutes and bluing. Dehydration, clearing, and microscopic examination were performed, and positive staining areas were quantified using ImageJ software. Serum levels of alanine aminotransferase (ALT) and aspartate aminotransferase (AST) in mice were determined using commercial assay kits (Nanjing Jiancheng, China, C009-2-1 for ALT and C010-2-1 for AST) according to the manufacturer's protocol.

2.8 Determination of serum specific IgG, IgG1, and IgG2a antibody titers

The rCsCP1-3 antigen was coated at 50 μg per well and incubated overnight at 4°C in a humid chamber. Non-specific binding was blocked with 5% bovine serum albumin (BSA) at 37°C for 2 hours. Primary antibodies from mouse serum were added starting at a 1:200 dilution, followed by serial dilutions up to 1:51200, and incubated overnight at 4°C. After three washes with PBS-T (pH 7.4), HRP-conjugated goat anti-mouse IgG secondary antibodies (diluted 1:50000, 100 μL per well) were added (Sangon Biotech, Shanghai, China, China, catalog number D110087-0100) and incubated for 1 hour at 37°C. The plates were washed three times with PBST (pH 7.4), and the colorimetric substrate 3,3',5,5'-tetramethylbenzidine (TMB) (100 μL per well) was added for color development. The reaction was allowed to proceed for 10-15 minutes at room temperature in the dark, then stopped by adding 1M sulfuric acid (H_2SO_4) (100 μL per well). Absorbance at 450 nm was measured using a microplate reader (BioTek Synergy H1). The endpoint titer for specific IgG antibodies in infected serum was determined as the highest dilution at which the measured values approximated those of the negative control serum.

2.9 Splenocyte preparation and cytokine measurement

The effect of rCsCP1-3 on splenocyte viability was evaluated using the CCK-8 assay (APExBIO, USA, K1018). Splenocytes were isolated and seeded into 96-well plates at a density of 5×10^5 cells per well in a complete RPMI-1640 medium (containing 10% fetal bovine serum and 1% penicillin/streptomycin) (34). After 24 hours of incubation at 37°C in a 5% CO2 atmosphere, cells were treated with rCsCP1-3 at concentrations of 0, 12.5, 25, 50, 100, and 200 μg/mL (10 μL per well) for an additional 24 hours. The old medium was removed, and 10 μL of CCK-8 solution was added to each well, followed by incubation for 2 hours at 37°C in a 5% CO2 incubator. Cell viability was assessed by measuring absorbance at 450 nm using a microplate reader (BioTek Synergy H1), with cell viability expressed as a percentage. The optimal concentration for co-culture with splenocytes was determined to be 12.5 μg/mL (100 μL per well).

For cytokine measurement, splenocytes were seeded into 24-well plates at a density of 5×10^5 cells/mL (1 mL per well) and treated with rCsCP1-3 at a concentration of 12.5 μg/mL (100 μL per well), with PBS serving as the negative control. After 48 hours of incubation at 37°C in a 5% CO2 environment, cell supernatants were collected and stored at -80°C for subsequent analysis. The concentrations of interleukin (IL)-2 (Multi Sciences, China, EK202), IL-4 (Multi Sciences, China, EK204), IL-10 (Multi Sciences, China, EK210), and interferon (IFN)-γ (Multi Sciences, China, EK280) in the supernatants were quantified using ELISA kits according to the manufacturer's protocol. A multifunctional microplate reader (BioTek Synergy H1) was used to measure dual-wavelength absorbance at 450 nm and 570 nm/630 nm, with the adjusted OD values calculated by subtracting the 570 nm/630 nm readings from the 450 nm readings. The experiment was performed in triplicate, and mean values were used for analysis.

2.10 Statistical analysis

All quantitative data are presented as mean ± standard deviation (x ± s) from three independent experiments. Data were analyzed using one-way analysis of variance (ANOVA), followed by Bonferroni's *post hoc* test. Statistical charts were generated using GraphPad Prism software (version 9.0; GraphPad Software, Inc.), and statistical analyses were conducted with SPSS software (version 25.0; SPSS Inc.).

3 Results

3.1 Sequence comparison and analysis

CsCP1-3 possess conserved structural domains characteristic of cysteine proteases, including ERFNIN, GNFD, GCNGG, and the catalytic triad C, H, N (Figure 1A). The open reading frame (ORF) amino acid sequences of CsCP1-3 are 326, 371, and 327 amino acids in length, respectively. The amino acid sequence homology between CsCP1 and CsCP2 is 52.9%, between CsCP1 and CsCP3 is 73.15%, and between CsCP2 and CsCP3 is 50.72%. Phylogenetic analysis of *C. sinensis* cysteine proteases reveals that CsCP1, CsCP2, and CsCP3 are situated on distinct branches (Figure 1B). B-cell epitope prediction, performed using the IEDB tool (https://www.iedb.org/), identified multiple phosphorylation sites and B-cell epitopes across CsCP1-3, suggesting strong antigenicity and immunogenicity, making CsCP1-3 a promising candidate for vaccine development (Supplementary Figure 1).

3.2 Expression of rCsCP1-3

The cDNA of CsCP1-3 from *C. sinensis* was cloned into the pPic9k expression vector. The recombinant proteins, expressed in *Pichia pastoris* GS115, were present in the soluble fraction. The

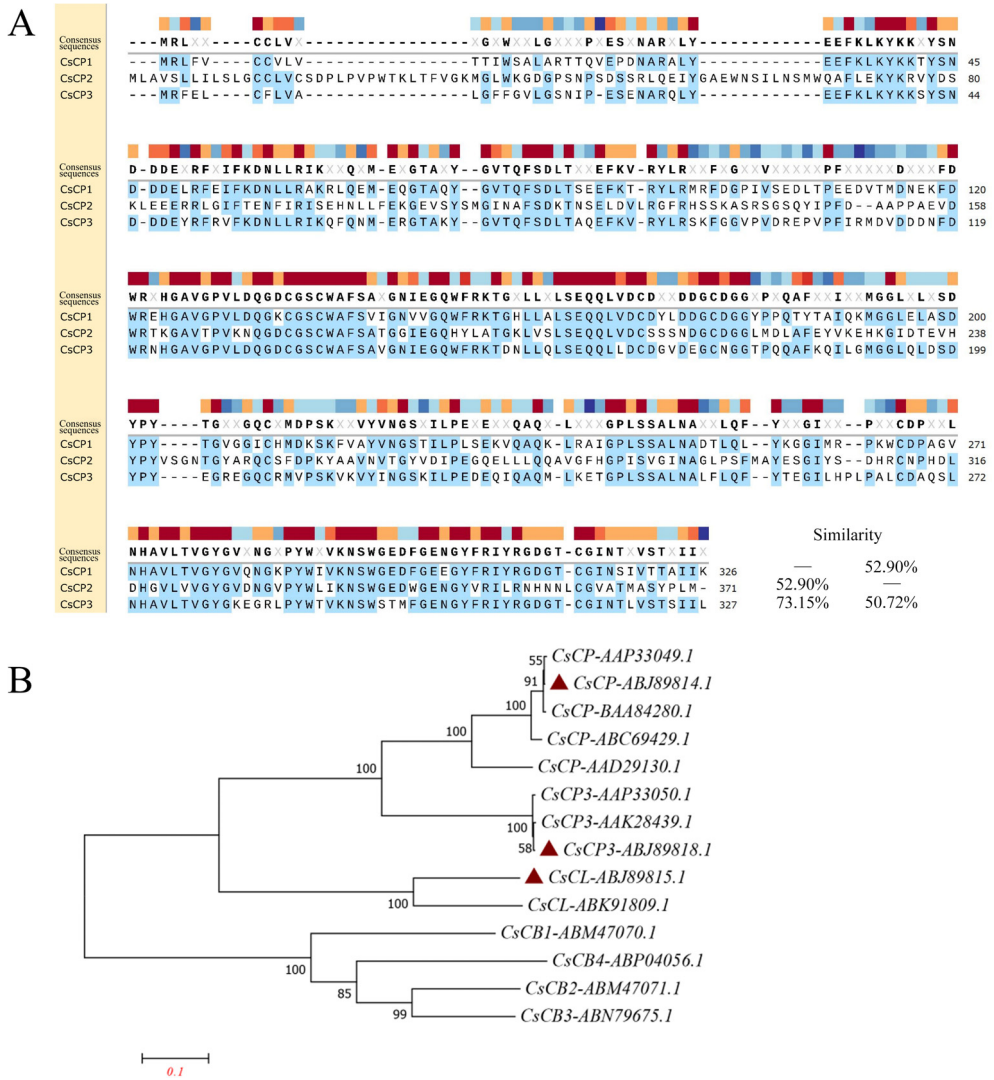

FIGURE 1
Homology and phylogenetic analysis of rCsCP1-3. **(A)** Homology analysis of the amino acid sequences of rCsCP1-3 revealed that all three proteins contain the conserved cysteine protease sequences ERFNIN, GNFD, and GCNGG, along with the catalytic residues C, H, and N. **(B)** Phylogenetic analysis of the amino acid sequences of rCsCP1-3 shows their clustering into distinct clades, with rCsCP1 and rCsCP3 being closely related. rCsCP1: ABJ89814.1; rCsCP2: ABJ89815.1; rCsCP3: ABJ89818.1.

soluble proteins were denatured with guanidine hydrochloride and purified using Ni2+-affinity chromatography (Figure 2A). The recombinant CsCP1-3 proteins were efficiently eluted at molecular weights of 35 kDa, 40 kDa, and 35 kDa, respectively. Western blot analysis confirmed that the target bands in the 72-hour induced supernatant were recognized by anti-6 × His monoclonal antibody (Figure 2B).

3.3 Transcriptional levels of CsCP1-3 at the egg, metacercaria, newly excysted juvenile, and adult worm stages

RT-qPCR results demonstrated that the expression of CsCP1 was significantly upregulated at the NEJ stage compared to the egg, metacercaria, and adult stages ($P < 0.001$), with expression in the NEJ stage being nearly 100-fold higher than in the other stages (Figure 3A). CsCP2 also exhibited the highest expression in the NEJ stage, being twice as high as in the adult and four times as high as in the egg stage (Figure 3B). In contrast, CsCP3 expression progressively increased across all stages, peaking in the adult worm stage (Figure 3C). These results suggest that CsCP1-3 have distinct roles throughout the developmental stages of *C. sinensis*.

3.4 Tissue localization of CsCP1-3 at different developmental stages of *C. sinensis*

Immunofluorescence localization revealed that CsCP1 is primarily localized on the surface of the eggshell, the surface of metacercariae, the tegument and oral sucker of NEJ, and the

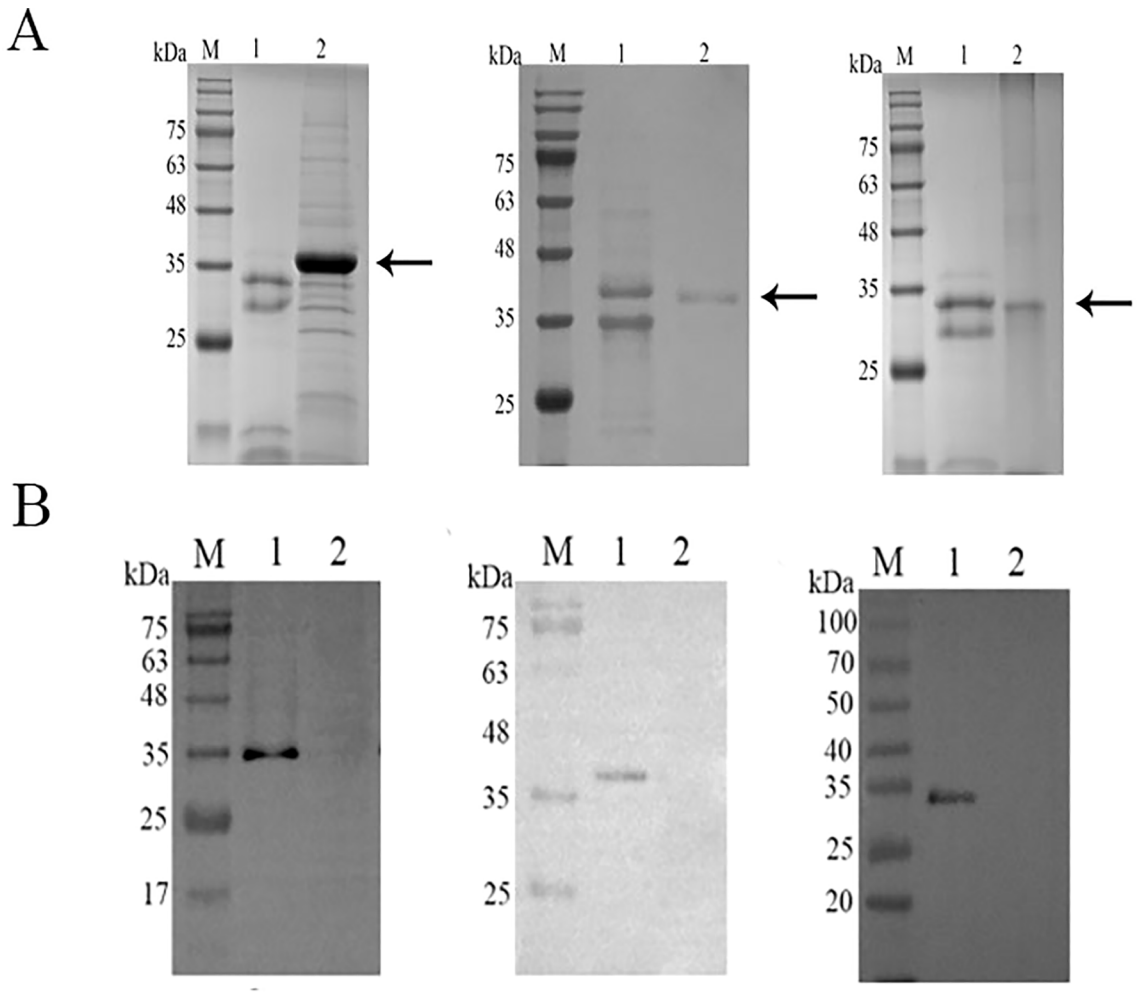

FIGURE 2
Expression and validation of rCsCP1-3 in yeast. **(A)** SDS-PAGE analysis of rCsCP1-3 purified using a nickel column (Ni-NTA), showing molecular weights of 35 kDa (rCsCP1 and rCsCP3) and 40 kDa (rCsCP2). **(B)** Western blotting of the 6 × His tag on rCsCP1-3. **(A, B)** show, from left to right, rCsCP1, rCsCP2, and rCsCP3; M, molecular weight markers; lane 1, induced protein expression of rCsCP1-3; lane 2, negative control.

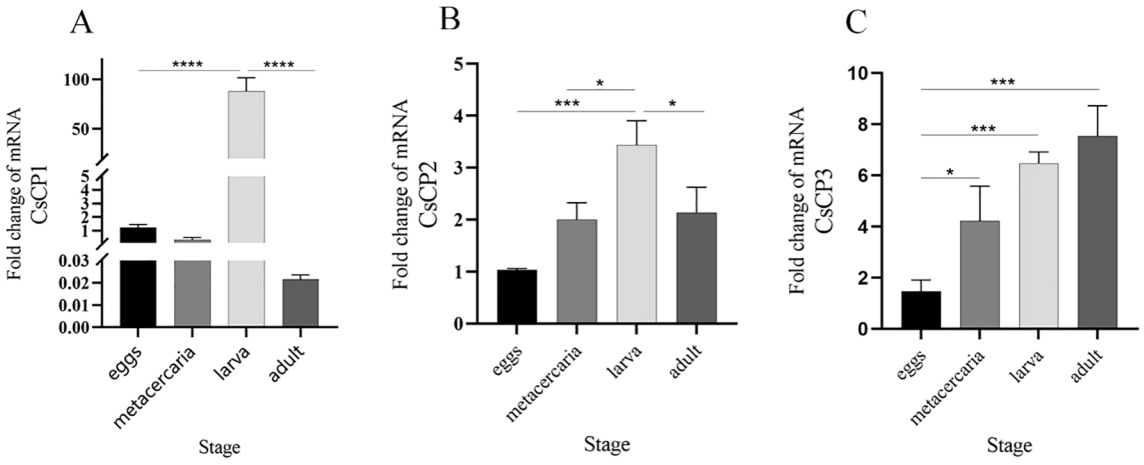

FIGURE 3
Gene expression of rCsCP1-3 at different developmental stages of *Clonorchis sinensis*. RT-qPCR was used to quantify the mRNA expression levels of rCsCP1-3 in the egg, metacercaria, newly excysted juvenile, and adult stages of *C. sinensis*. **(A)** rCsCP1; **(B)** rCsCP2; **(C)** rCsCP3. *P < 0.05, **P < 0.01, ***P < 0.001, ****P < 0.0001.

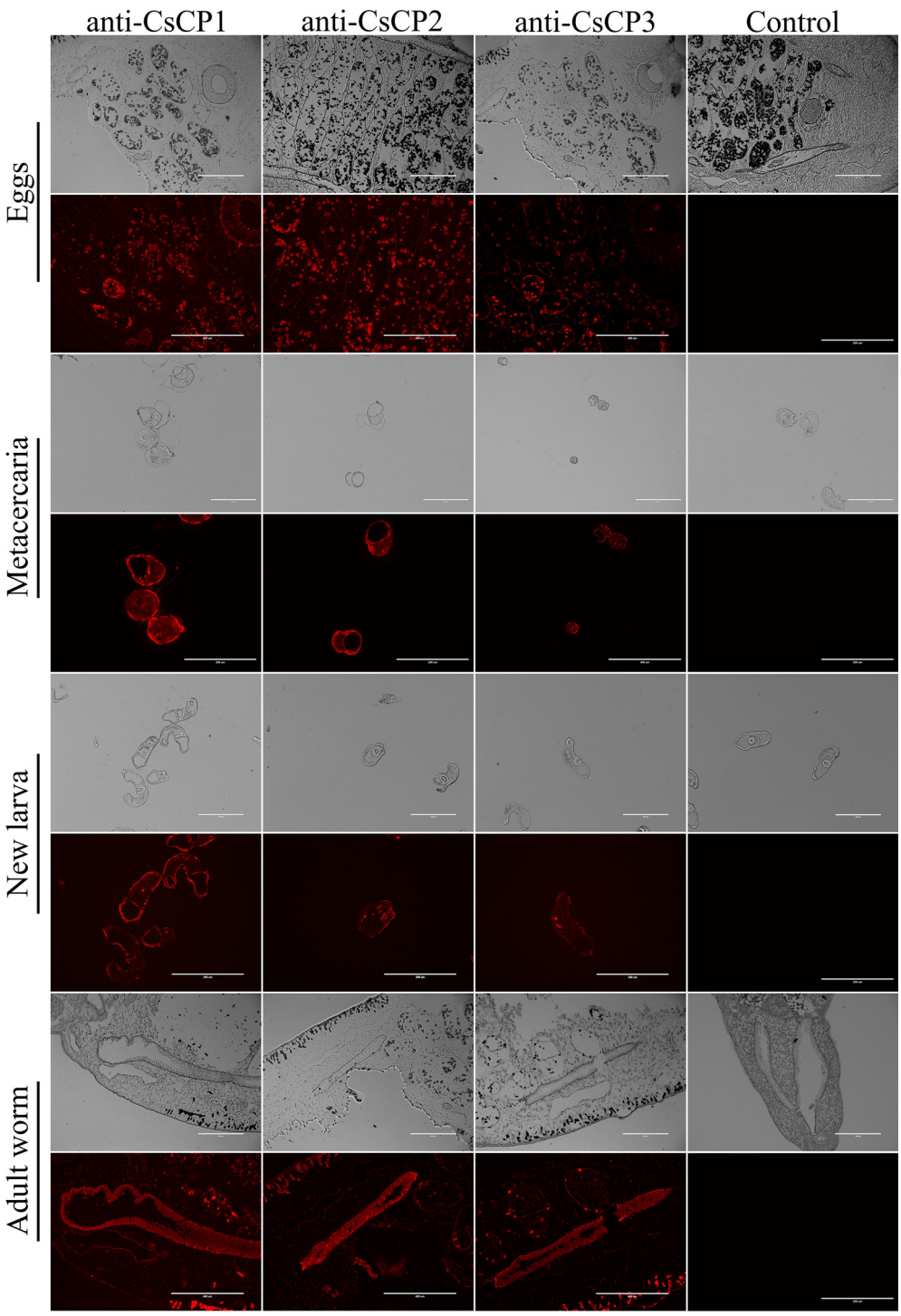

FIGURE 4
Tissue localization of rCsCP1-3 at various developmental stages of *Clonorchis sinensis*. Immunofluorescence localization of rCsCP1-3 distribution in eggs, metacercariae, newly excysted juveniles, and adult stages of *Clonorchis sinensis*.

intestine, tegument, and cell layer of adult worms (Figure 4). CsCP2 and CsCP3 are predominantly found on the eggshell and metacercariae surfaces, the tegument of NEJ, and the intestine, body surface tegument, and cell layers of adult worms (Figure 4). No fluorescence signal was detected in the PBS-immunized rat serum, which served as a negative control (Figure 4).

3.5 Examination of liver tissue sections stained

Infection experiments demonstrated that mice immunized with rCsCP1-3, as well as those in the PBS and PBS plus Freund's adjuvant groups, exhibited mild liver lesions one month after being

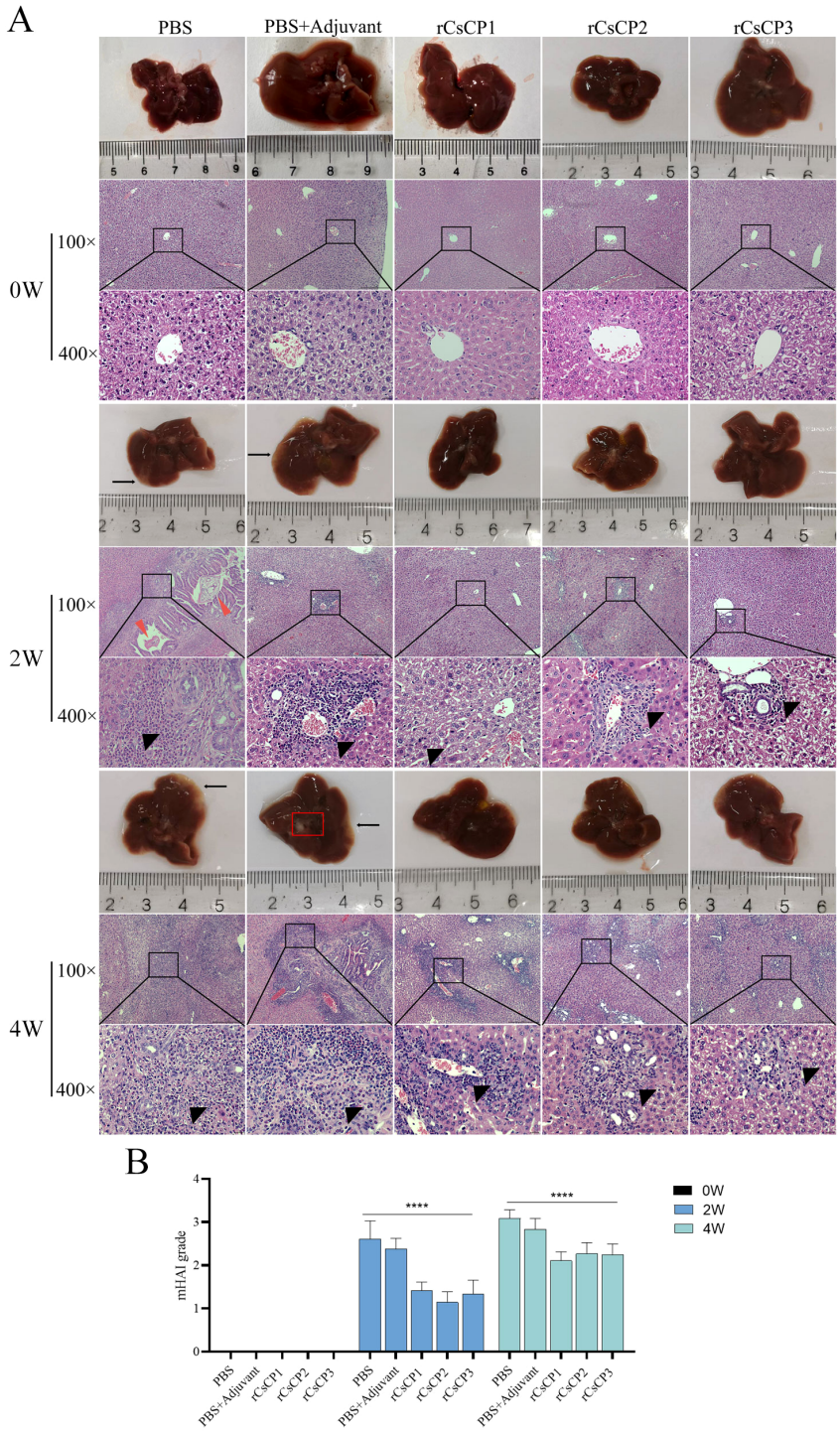

FIGURE 5
rCsCP1-3 immunization ameliorates liver damage and inflammatory infiltration induced by *Clonorchis sinensis* infection in mice. Mice immunized with rCsCP1-3 exhibited no significant pathological changes in liver morphology. In contrast, liver samples from PBS and PBS plus Freund's adjuvant-treated groups showed increased lesion sites and the formation of small cysts **(A)**. H&E staining revealed dense inflammatory cell infiltration around bile duct tissues in the PBS and PBS plus Freund's adjuvant groups compared to the rCsCP1-3 immunized group **(A)**. The degree of liver pathology in each group was assessed using the mHAI scoring system **(B)**. Note: Black arrows indicate small cysts; black triangles indicate inflammatory infiltration; red triangles indicate *C.s sinensis* juvenile worms; ****P < 0.0001. Scale bar: 100 μm.

challenged with *C. sinensis* metacercariae, with no significant gross appearance differences. However, H&E staining revealed a substantial influx of neutrophils and lymphocytes from the bile ducts to the surrounding tissues in the PBS and PBS plus Freund's adjuvant groups (Figure 5A). In contrast, in mice vaccinated with rCsCP1-3, the inflammatory cell infiltration around the bile ducts was less pronounced (Figure 5A), indicating a milder degree of liver inflammation. Moreover, mHAI scores for the PBS and PBS plus Freund's adjuvant groups were significantly higher than those for the rCsCP1-3 immunized group at both the second and fourth weeks post-infection ($P < 0.001$) (Figure 5B), suggesting that rCsCP1-3 immunization resulted in reduced hepatic inflammation.

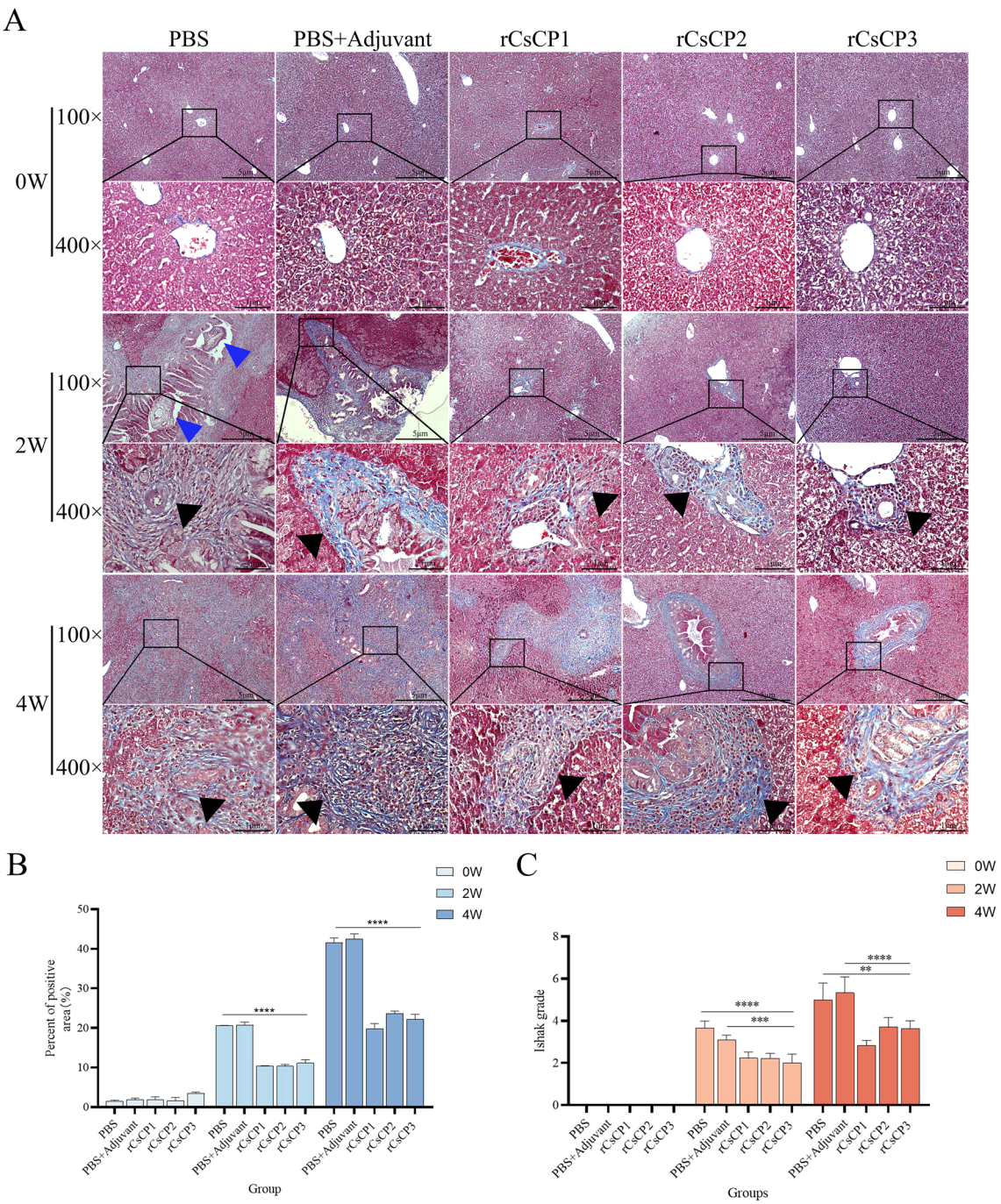

FIGURE 6
rCsCP1-3 immunization ameliorates fibrosis induced by *Clonorchis sinensis* infection. Fixed liver tissues were assessed for collagen deposition using Masson's trichrome staining (blue indicates collagen deposition areas). Infection with *Clonorchis sinensis* resulted in significant collagen deposition in bile duct areas, which was alleviated by immunization with rCsCP1-3 proteins **(A)**. Hepatic fibrosis was quantified using ImageJ **(B)** and the Ishak scoring system **(C)**. Blue triangles indicate *C. sinensis* juvenile worms; black triangles indicate collagen deposition areas. **P < 0.01, ***P < 0.001, ****P < 0.0001; Scale bar: 100 μm.

Masson's staining of liver tissues showed a reduction in collagen fiber proliferation in the bile duct areas of the rCsCP1-3 immunized group compared to the PBS and PBS plus Freund's adjuvant groups (Figure 6A), accompanied by a decrease in fibrotic area (Figure 6A). ImageJ analysis and Ishak scoring indicated that the rCsCP1-3 immunized group had significantly lower scores than the PBS and PBS plus Freund's adjuvant groups at both the second and fourth weeks post-infection (Figures 6B, C). These results consistently demonstrated a lower degree of liver fibrosis in the rCsCP1-3 immunized group.

Immunohistochemical analysis showed that the expression of α-SMA and Collagen I in the rCsCP1-3 immunized group was lower than in the PBS and PBS plus Freund's adjuvant groups (Figures 7A, C). Statistical analysis of the positive staining areas confirmed that α-SMA and Collagen I expression was significantly reduced in the rCsCP1-3 immunized group compared to the PBS and PBS plus Freund's adjuvant groups ($P < 0.05$) (Figures 7B, D). These results suggest that rCsCP1-3 immunization alleviates biliary damage and fibrosis in mice following *C. sinensis* infection.

3.6 Anti-rCsCP1-3 IgG antibody titer assay

Antibody titer assays demonstrated that immunization with rCsCP1-3 induced a rapid production of specific IgG within two weeks post-infection, whereas no increase was observed in control groups receiving adjuvant or PBS (Figure 8A). Analysis of IgG subclasses, IgG1 and IgG2a, revealed a rapid rise in IgG1 levels in the rCsCP1 immunized group, with a deceleration in the second week. IgG2a exhibited a gradual increase in the first two weeks,

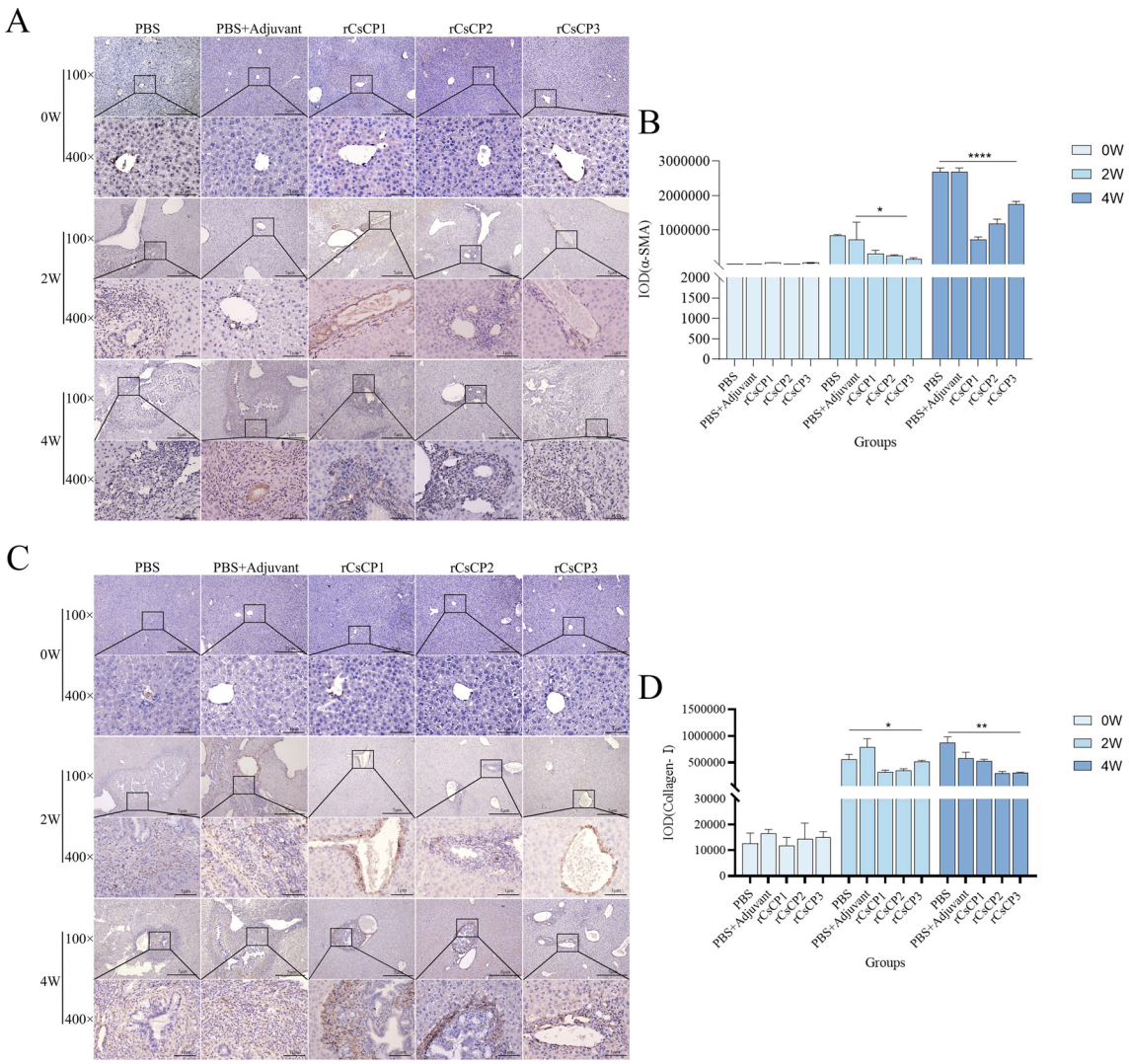

FIGURE 7
rCsCP1-3 immunization reduces the expression of α-SMA and anti-Collagen-I in *Clonorchis sinensis*-infected mouse liver tissues. Fixed liver tissues were stained with anti-α-SMA **(A)** and anti-Collagen-I **(C)** antibodies. The positive staining areas were quantified using ImageJ **(B, D)**. Following *Clonorchis sinensis* infection, α-SMA and Collagen-I staining intensity increased in the PBS and PBS plus Freund's adjuvant groups. In contrast, the rCsCP1-3 immunized group exhibited reduced staining intensity. The brown patr represents positive areas; *P < 0.05, **P < 0.01, ***P < 0.001, ****P < 0.0001. Scale bar: 100 μm.

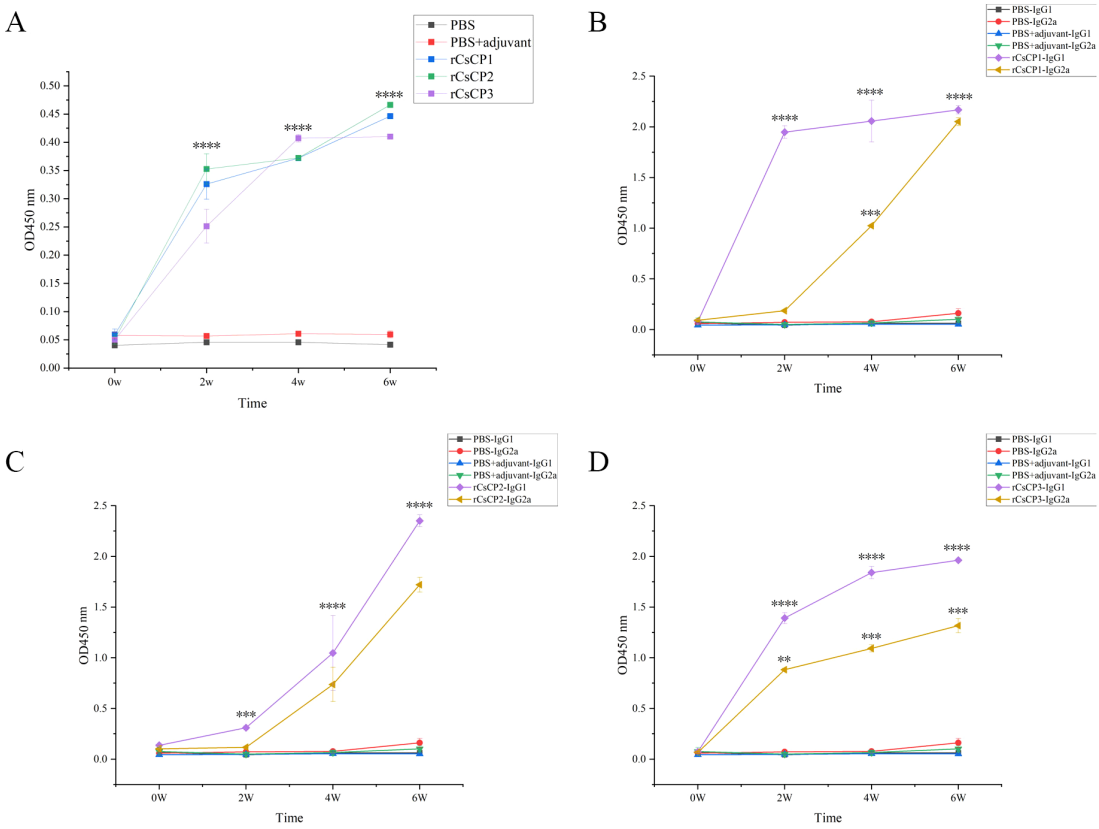

FIGURE 8
Specific IgG antibody levels induced by rCsCP1-3 immunization. Immunization with rCsCP1-3 rapidly induced specific IgG production **(A)**, including subclasses IgG1 **(B)** and IgG2a **(C, D)**. **P < 0.01, ***P < 0.001, ****P < 0.0001.

followed by a sharp rise (Figure 8B). In the rCsCP2 immunized group, both IgG1 and IgG2a titers showed a steady increase in the first two weeks, with a rapid escalation thereafter (Figure 8C). In contrast, the rCsCP3 immunized group displayed an initial rapid increase in both IgG1 and IgG2a titers, followed by a decelerated rate of increase in the second week (Figure 8D).

3.7 Measurement of cytokine levels

ELISA results indicated that in the rCsCP1 immunized group, IL-10 levels surged over 10-fold (11.73 ± 1.97)by the first week post-infection, compared to control groups, and remained elevated at the second week. Concurrently, IFN-γ, IL-2, and IL-4 increased significantly starting from the second week ($P < 0.001$), with IFN-γ expression being more than 80-fold(82.93 ± 12.86) higher than in control groups (Figure 9). In the rCsCP2 immunized group, IL-2 and IL-4 levels rose from the second and fourth weeks post-infection, while IFN-γ levels decreased noticeably, and IL-10 expression remained unchanged compared to controls (Figure 9). In the rCsCP3 immunized group, IFN-γ, IL-2, and IL-10 were elevated from the first week post-infection (P < 0.01), with IL-4 levels increasing in the second week. By the fourth week, no significant differences in the expression of IFN-γ, IL-2, IL-4, or IL-10 were observed between the immunized and control groups (Figure 9).

4 Discussion

This study revealed three key characteristics of CsCP1-3. Both CsCP1 and CsCP2 exhibit the highest expression in the NEJ stage, with CsCP1 showing over 200 times higher expression than in the adult and metacercarial stages. This suggests that CsCP1 may play a critical role in key processes during the NEJ stage, such as excystation, intestinal invasion, and nutrient absorption. Further analysis demonstrated that CsCP1 is widely distributed on the eggshell, the surface of metacercariae, the outer tegument and oral sucker of NEJ, as well as the intestine, tegument, and cell layers of adult worms. The outer tegument proteins have been shown to interact directly with immune cells, antibodies, and cytokines (35), and several tegumental proteins have been identified as potential vaccine candidates in flukes (28, 36, 37).

To evaluate the immunoprotective effects of CsCP1-3 following *C. sinensis* challenge and two booster immunizations, liver damage was assessed using hematoxylin and eosin (HE) staining, Masson's trichrome staining, and immunohistochemical analysis of α-smooth muscle actin (α-SMA) and Collagen-I. Post-immunization results indicated that CsCP1-3 effectively reduced liver fibrosis progression and inflammatory cell infiltration. Compared to the CsCP1-3 immunized group, control mice displayed thicker bile ducts, more pronounced collagen fiber proliferation in the bile duct area, and higher

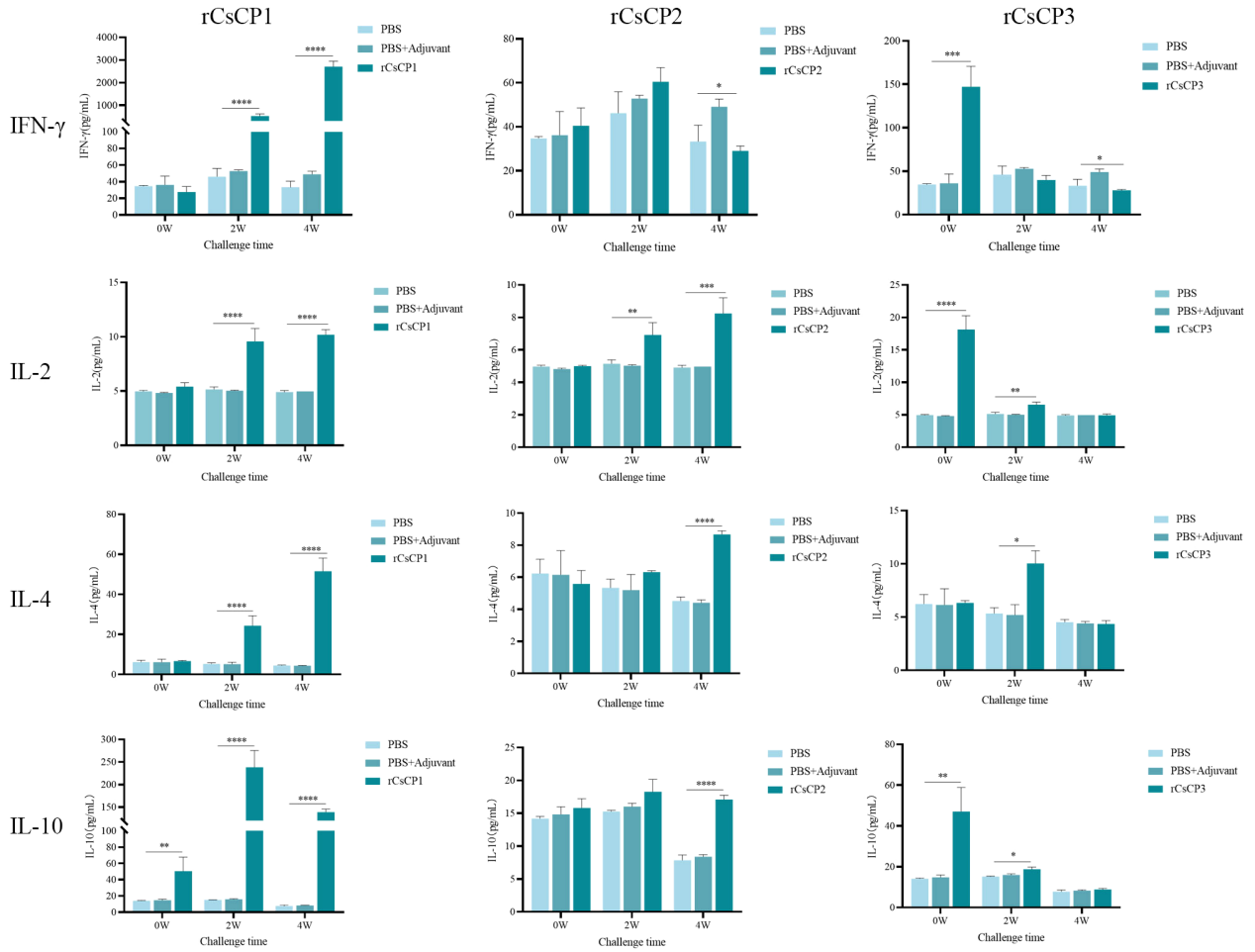

FIGURE 9
Cytokine secretion levels of IFN-γ, IL-2, IL-4, and IL-10. Compared to the PBS and PBS plus Freund's adjuvant control groups, the rCsCP1-immunized group showed a sharp increase in IL-10, IFN-γ, IL-2, and IL-4 levels within two weeks. The rCsCP2-immunized group induced a gradual increase in IFN-γ, IL-4, and IL-10 levels within four weeks. The rCsCP3-immunized group showed an initial increase in IFN-γ, IL-2, IL-4, and IL-10 levels within two weeks, followed by a rapid decrease, with no significant differences compared to the control groups. **P < 0.01, ***P < 0.001, ****P < 0.0001.

levels of α-SMA and Collagen-I. These findings suggest that immunization with CsCP1-3 significantly mitigated liver tissue damage and reduced liver fibrosis induced by *C. sinensis* infection.

To preliminarily investigate the immunoprotective mechanisms of CsCP1-3, antibody and cytokine responses were evaluated following immunization. Immunization with CsCP1-3 induced a rapid production of IgG, with IgG subclasses IgG1 and IgG2a showing a gradual increase from 1 to 4 weeks post-infection. Previous studies on potential vaccine candidates for *C. sinensis* have linked protective immunity and worm reduction to elevated levels of IgG1/IgG2a (36, 38). Cytokine analysis revealed that the levels of IFN-γ, IL-2, IL-4, and IL-10 were significantly higher in the CsCP1-immunized group compared to the control group, particularly IFN-γ and IL-10, which were more than 10 times higher than in controls. IL-10, an important anti-inflammatory cytokine, plays a pivotal role in fibrosis and is primarily secreted by activated macrophages and dendritic cells, exerting inhibitory effects on fibrosis (39, 40). In *C. sinensis*-infected mice, serum cytokines IL-4 and IL-10 increased, with IL-10 showing a marked rise (41), while IFN-γ and IL-2 levels decreased. During liver fibrosis, Polarized macrophages release anti-inflammatory factor IL-10, influencing fibrosis progression (42). Moreover, IL-10 gene therapy has been shown to reverse thioacetamide-induced liver fibrosis in mice (43). The increased levels of IgG1/IgG2a antibodies and cytokines IFN-γ, IL-2, IL-4, and IL-10 following CsCP1 immunization suggest that CsCP1 elicits a mixed type 1/type 2 immune response, mitigating liver damage caused by *C. sinensis* infection. In previous studies, vaccine candidates for *C. sinensis* have achieved significant worm reduction and alleviated liver damage by inducing a mixed type 1/type 2 immune response (36, 44, 45).

In the CsCP2-immunized group, IgG1/IgG2a levels gradually increased, and IL-2 and IL-4 expression significantly surpassed that of the control group at four weeks post-infection. This suggests that CsCP2 also triggers a mixed type 1/type 2 immune response in the adult stage, reducing liver damage. In the CsCP3-immunized group, expression levels of IFN-γ, IL-2, IL-4, and IL-10 rose rapidly post-infection but subsequently dropped to levels not significantly

different from the control by the second or fourth week. This suggests that the observed reduction in liver damage is likely attributed to a robust innate immune response, which is critical in triggering the subsequent adaptive immune response (46, 47).

5 Conclusion

This study characterized the expression and localization of three cysteine proteases (CsCP1-3) from *C. sinensis* across various life cycle stages of the parasite. Immunization with CsCP1-3 effectively reduced liver damage caused by *C. sinensis* infection, although the protective mechanisms varied among the three proteins. Notably, CsCP1 elicited a robust mixed type 1/type 2 immune response, highlighting its potential as a vaccine candidate. Future research will focus on detailed vaccine efficacy, including worm burden reduction rates and further exploration of the underlying protective mechanisms.

Data availability statement

The datasets presented in this study can be found in online repositories. The names of the repository/repositories and accession number(s) can be found in the article/Supplementary Material.

Ethics statement

The animal study was approved by Committee on Ethics of Animal Experiments, Guangxi Medical University (Approval Number: 202201015 and 202201016). The study was conducted in accordance with the local legislation and institutional requirements.

Author contributions

YS: Investigation, Methodology, Validation, Writing – original draft, Writing – review & editing, Conceptualization, Visualization, Formal Analysis. XL: Data curation, Formal Analysis, Investigation, Writing – original draft, Software. KL: Data curation, Formal Analysis, Investigation, Writing – original draft. TL: Data curation, Formal Analysis, Investigation, Writing – original draft. YC: Data curation, Formal Analysis, Investigation, Writing – review & editing. YSL: Conceptualization, Data curation, Formal Analysis, Writing – original draft. YTL: Data curation, Investigation, Writing – original draft. SW: Data curation, Investigation, Writing – original draft. SH: Data curation, Investigation, Writing – original draft. LT: Data curation, Investigation, Writing – original draft. DL: Conceptualization, Formal Analysis, Supervision, Writing – review & editing. YWL: Conceptualization, Formal Analysis, Funding acquisition, Investigation, Writing – review & editing, Supervision, Writing – original draft, Project administration, Validation.

Funding

The author(s) declare that financial support was received for the research and/or publication of this article. This work was supported by the Joint Funds of the Natural Science Foundation of Guangxi Zhuang Autonomous Region (2019GXNSFAA245069, 2020GXNSFAA159068).

Conflict of interest

The authors declare that the research was conducted in the absence of any commercial or financial relationships that could be construed as a potential conflict of interest.

Generative AI statement

The author(s) declare that no Generative AI was used in the creation of this manuscript.

Publisher's note

Supplementary material

The Supplementary Material for this article can be found online at: https://www.frontiersin.org/articles/10.3389/fimmu.2025.1550775/full#supplementary-material

References

1. Hong ST, Fang Y. *Clonorchis sinensis* and clonorchiasis, an update. *Parasitol Int*. (2012) 61:17–24. doi: 10.1016/j.parint.2011.06.007

2. Zhu TJ, Chen YD, Qian MB, Zhu HH, Huang JL, Zhou CH, et al. Surveillance of clonorchiasis in China in 2016. *Acta Trop*. (2020) 203:105320. doi: 10.1016/j.actatropica.2019.105320

3. Bouvard V, Baan R, Straif K, Grosse Y, Secretan B, El ghissassi F, et al. A review of human carcinogens–Part B: biological agents. *Lancet Oncol*. (2009) 10:321–2. doi: 10.1016/s1470-2045(09)70096-8

4. Kim TS, Pak JH, Kim JB, Bahk YY. *Clonorchis sinensis*, an oriental liver fluke, as a human biological agent of cholangiocarcinoma: a brief review. *BMB Rep*. (2016) 49:590–7. doi: 10.5483/bmbrep.2016.49.11.109

5. Na BK, Pak JH, Hong SJ. *Clonorchis sinensis* and clonorchiasis. *Acta Trop*. (2020) 203:105309. doi: 10.1016/j.actatropica.2019.105309

6. Qian MB, Utzinger J, Keiser J, Zhou XN. Clonorchiasis. *Lancet*. (2016) 387:800–10. doi: 10.1016/s0140-6736(15)60313-0

7. Tang ZL, Huang Y, Yu XB. Current status and perspectives of *Clonorchis sinensis* and clonorchiasis: epidemiology, pathogenesis, omics, prevention and control. *Infect Dis Poverty*. (2016) 5:71. doi: 10.1186/s40249-016-0166-1

8. Qian MB, Keiser J, Utzinger J, Zhou XN. Clonorchiasis and opisthorchiasis: epidemiology, transmission, clinical features, morbidity, diagnosis, treatment, and control. *Clin Microbiol Rev*. (2024) 37:e0000923. doi: 10.1128/cmr.00009-23

9. Yao JK, Dai JR. The epidemiology of clonorchiasis and the status of its treatment. *J Pathogen Biol*. (2020) 15:364–70. doi: 10.13350/j.cjpb.200326

10. Grzonka Z, Jankowska E, Kasprzykowski F, Kasprzykowska R, Lankiewicz L, Wiczk W, et al. Structural studies of cysteine proteases and their inhibitors. *Acta Biochim Pol*. (2001) 48:1–20. doi: 10.18388/abp.2001_5108

11. Siqueira-neto JL, Debnath A, Mccall LI, Bernatchez JA, Ndao M, Reed SL, et al. Cysteine proteases in protozoan parasites. *PloS Negl Trop Dis*. (2018) 12:e0006512. doi: 10.1371/journal.pntd.0006512

12. Grote A, Caffrey CR, Rebello KM, Smith D, Dalton JP, Lustigman S. Cysteine proteases during larval migration and development of helminths in their final host. *PloS Negl Trop Dis*. (2018) 12:e0005919. doi: 10.1371/journal.pntd.0005919

13. Yang N, Matthew MA, Yao C. Roles of cysteine proteases in biology and pathogenesis of parasites. *Microorganisms*. (2023) 11:1937. doi: 10.3390/microorganisms11061397

14. Villa-mancera A, Alcalá-canto Y, Olivares-pérez J, Molina-mendoza P, Hernández-guzmán K, Utrera-quintana F, et al. Vaccination with cathepsin L mimotopes of *Fasciola hepatica* in goats reduces worm burden, morphometric measurements, and reproductive structures. *Microb Pathog*. (2021) 155:104859. doi: 10.1016/j.micpath.2021.104859

15. Tallima H, Abou El Dahab M, El Ridi R. Role of T lymphocytes and papain enzymatic activity in the protection induced by the cysteine protease against *Schistosoma mansoni* in mice. *J Adv Res*. (2019) 17:73–84. doi: 10.1016/j.jare.2018.12.008

16. Tallima H, Dvořák J, Kareem S, Abou el dahab M, Abdel aziz N, Dalton JP, et al. Protective immune responses against *Schistosoma mansoni* infection by immunization with functionally active gut-derived cysteine peptidases alone and in combination with glyceraldehyde 3-phosphate dehydrogenase. *PloS Negl Trop Dis*. (2017) 11:e0005443. doi: 10.1371/journal.pntd.0005443

17. Bakshi M, Tuo W, Aroian RV, Zarlenga D. Immune reactivity and host modulatory roles of two novel *Haemonchus contortus* cathepsin B-like proteases. *Parasit Vectors*. (2021) 14:580. doi: 10.1186/s13071-021-05010-y

18. Liu RD, Meng XY, Le L i C, Xu QY, Lin XZ, Dong BR, et al. *Trichinella spiralis* cathepsin L induces macrophage M1 polarization via the NF-κB pathway and enhances the ADCC killing of newborn larvae. *Parasit Vectors*. (2023) 16:433. doi: 10.1186/s13071-023-06051-1

19. Quan FS, Matsumoto T, Lee JB, Timothy O, Kim TS, Joo KH, et al. Immunization with *Trichinella spiralis* Korean isolate larval excretory-secretory antigen induces protection and lymphocyte subset changes in rats. *Immunol Invest*. (2004) 33:15–26. doi: 10.1081/imm-120027681

20. Chaimon S, Limpanont Y, Reamtong O, Ampawong S, Phuphisut O, Chusongsang P, et al. Molecular characterization and functional analysis of the *Schistosoma mekongi* Ca(2+)-dependent cysteine protease (calpain). *Parasit Vectors*. (2019) 12:383. doi: 10.1186/s13071-019-3639-9

21. Tang Z, Wu Z, Sun H, Zhao L, Shang M, Shi M, et al. The storage stability of Bacillus subtilis spore displaying cysteine protease of *Clonorchis sinensis* and its effect on improving the gut microbiota of mice. *Appl Microbiol Biotechnol*. (2021) 105:2513–26. doi: 10.1007/s00253-021-11126-z

22. Ju JW, Joo HN, Lee MR, Cho SH, Cheun HI, Kim JY, et al. Identification of a serodiagnostic antigen, legumain, by immunoproteomic analysis of excretory-secretory products of *Clonorchis sinensis* adult worms. *Proteomics*. (2009) 9:3066–78. doi: 10.1002/pmic.200700613

23. Kang JM, Bahk YY, Cho PY, Hong SJ, Kim TS, Sohn WM, et al. A family of cathepsin F cysteine proteases of *Clonorchis sinensis* is the major secreted proteins that are expressed in the intestine of the parasite. *Mol Biochem Parasitol*. (2010) 170:7–16. doi: 10.1016/j.molbiopara.2009.11.006

24. Chen W, Ning D, Wang X, Chen T, Lv X, Sun J, et al. Identification and characterization of *Clonorchis sinensis* cathepsin B proteases in the pathogenesis of clonorchiasis. *Parasit Vectors*. (2015) 8:647. doi: 10.1186/s13071-015-1248-9

25. Ma C, Liang K, Tang L, He S, Liu X, He M, et al. Identification and characteristics of a cathepsin L-like cysteine protease from. *Clonorchis sinensis Parasitol Res*. (2019) 118:829–35. doi: 10.1007/s00436-019-06223-y

26. Lee JS, Kim IS, Sohn WM, Lee J, Yong TS. Vaccination with DNA encoding cysteine proteinase confers protective immune response to rats infected with Clonorchis sinensis. *Vaccine*. (2006) 24:2358–66. doi: 10.1016/j.vaccine.2005.11.062

27. Tang Z, Shang M, Chen T, Ren P, Sun H, Qu H, et al. The immunological characteristics and probiotic function of recombinant Bacillus subtilis spore expressing Clonorchis sinensis cysteine protease. *Parasit Vectors*. (2016) 9:648. doi: 10.1186/s13071-016-1928-0

28. Tang Z, Sun H, Chen T, Lin Z, Jiang H, Zhou X, et al. Oral delivery of Bacillus subtilis spores expressing cysteine protease of Clonorchis sinensis to grass carp (Ctenopharyngodon idellus): Induces immune responses and has no damage on liver and intestine function. *Fish Shellfish Immunol*. (2017) 64:287–96. doi: 10.1016/j.fsi.2017.03.030l

29. Wu Y, Deng X, Wu Z, Liu D, Fu X, Tang L, et al. Multilayer omics reveals the molecular mechanism of early infection of *Clonorchis sinensis* juvenile. *Parasit Vectors*. (2023) 8:285. doi: 10.1186/s13071-023-05891-1

30. Li Q, Li X, Kan S, Zhu TJ, Li C, Du XY, et al. *Clonorchis sinensis* calcium-binding protein Cs16 causes acute hepatic injury possibly by reprogramming the metabolic pathway of bone marrow-derived monocytes. *Front Cell Infect Microbiol*. (2023) 10:1280358. doi: 10.3389/fcimb.2023.1280358

31. Livak KJ, Schmittgen TD. Analysis of relative gene expression data using real-time quantitative PCR and the 2(-Delta Delta C(T)) Method. *Methods*. (2001) 12:402–8. doi: 10.1006/meth.2001.1262

32. Chevallier M, Guerret S, Chossegros P, Gerard F, Grimaud JA. A histological semiquantitative scoring system for evaluation of hepatic fibrosis in needle liver biopsy specimens: comparison with morphometric studies. *Hepatology*. (1994) 8:349–55. doi: 10.1002/(ISSN)1527-3350

33. Ishak K, Baptista A, Bianchi L, Callea F, De Groote J, Gudat F, et al. Histological grading and staging of chronic hepatitis. *J Hepatol*. (1995) 6:696–9. doi: 10.1016/0168-8278(95)80226-6

34. Xu Y, Liang P, Bian M, Chen W, Wang X, Lin J, et al. Interleukin-13 is involved in the formation of liver fibrosis in *Clonorchis sinensis*-infected mice. *Parasitol Res*. (2016) 115:2653–60. doi: 10.1007/s00436-016-5012-7

35. Chung E, Kim YJ, Lee MR, Cho SH, Ju JW. A 21.6 kDa tegumental protein of *Clonorchis sinensis* induces a Th1/Th2 mixed immune response in mice. *Immun Inflammation Dis*. (2018) 6:435–47. doi: 10.1002/iid3.235

36. Lee DH, Kim AR, Lee SH, Quan FS. Virus-like particles vaccine containing *Clonorchis sinensis* tegumental protein induces partial protection against *Clonorchis sinensis* infection. *Parasit Vectors*. (2017) 10:626. doi: 10.1186/s13071-017-2526-5

37. Zhao L, Shi M, Zhou L, Sun H, Zhang X, He L, et al. *Clonorchis sinensis* adult-derived proteins elicit Th2 immune responses by regulating dendritic cells via mannose receptor. *PloS Negl Trop Dis*. (2018) 12:e0006251. doi: 10.1371/journal.pntd.0006251

38. Wang X, Chen W, Lv X, Tian Y, Men J, Zhang X, et al. Identification and characterization of paramyosin from cyst wall of metacercariae implicated protective efficacy against *Clonorchis sinensis* infection. *PloS One*. (2012) 7:e33703. doi: 10.1371/journal.pone.0033703

39. Yu B, Qin SY, Hu BL, Qin QY, Jiang HX, Luo W. Resveratrol improves CCL4-induced liver fibrosis in mouse by upregulating endogenous IL-10 to reprogramme macrophages phenotype from M(LPS) to M(IL-4). *BioMed Pharmacother*. (2019) 117:109110. doi: 10.1016/j.biopha.2019.109110

40. Xu Y, Tang X, Yang M, Zhang S, Li S, Chen Y, et al. Interleukin 10 gene-modified bone marrow-derived dendritic cells attenuate liver fibrosis in mice by inducing regulatory T cells and inhibiting the TGF-β/smad signaling pathway. *Mediators Inflamm*. (2019) 2019:4652596. doi: 10.1155/2019/4652596

41. Jin Y, Wi HJ, Choi MH, Hong ST, Bae YM. Regulation of anti-inflammatory cytokines IL-10 and TGF-β in mouse dendritic cells through treatment with Clonorchis sinensis crude antigen. *Exp Mol Med*. (2014) 46:e74. doi: 10.1038/emm.2013.144

42. Chang L, Gao J, Yu Y, Liao B, Zhou Y, Zhang J, et al. MMP10 alleviates non-alcoholic steatohepatitis by regulating macrophage M2 polarization. *Int Immunopharmacol*. (2023) 124:111045. doi: 10.1016/j.intimp.2023.111045

43. Hung KS, Lee TH, Chou WY, Wu CL, Cho CL, Lu CN, et al. Interleukin-10 gene therapy reverses thioacetamide-induced liver fibrosis in mice. *Biochem Biophys Res Commun*. (2005) 336:324–31. doi: 10.1016/j.bbrc.2005.08.085

44. Bai X, Song JH, Dai F, Lee JY, Hong SJ. *Clonorchis sinensis* secretory protein CsAg17 vaccine induces immune protection. *Parasit Vectors*. (2020) 13:215. doi: 10.1186/s13071-020-04083-5

45. Sun H, Lin Z, Zhao L, Chen T, Shang M, Jiang H, et al. Bacillus subtilis spore with surface display of paramyosin from *Clonorchis sinensis* potentializes a promising oral vaccine candidate. *Parasit Vectors*. (2018) 11:156. doi: 10.1186/s13071-018-2757-0

46. Heymann F, Tacke F. Immunology in the liver–from homeostasis to disease. *Nat Rev Gastroenterol Hepatol*. (2016) 13:88–110. doi: 10.1038/nrgastro.2015.200

47. Kubes P, Jenne C. Immune responses in the liver. *Annu Rev Immunol*. (2018) 36:247–77. doi: 10.1146/annurev-immunol-051116-052415